 CMES, vol.15, no.3, pp.179-196, 2006

The Lie-Group Shooting Method for Singularly Perturbed Two-Point Boundary Value Problems

Chein-Shan Liu[1]

Abstract: This paper studies the numerical computations of the second-order singularly perturbed boundary value problems (SPBVPs). In order to depress the singularity we consider a coordinate transformation from the x-domain to the t-domain. The relation between singularity and stiffness is demonstrated, of which the coordinate transformation parameter λ plays a key role to balance these two tendencies. Then we construct a very effective Lie-group shooting method to search the missing initial condition through a weighting factor $r \in (0,1)$ in the t-domain formulation. For stabilizing the new method we also introduce two new systems by a translation of the dependent variable. Numerical examples are examined to show that the new approach has high efficiency and high accuracy. Only through a few trials one can determine a suitable r very soon, and the new method can attain the second-order accuracy even for the highly singular cases. A finite difference method together with the nonstandard group preserving scheme for solving the resulting ill-posed equations is also provided, which is a suitable method for the calculations of SPBVPs without needing for many grid points. This method has the first-order accuracy.

keyword: One-step group preserving scheme, Singularly perturbed boundary value problem, Boundary layer, Lie-group shooting method, Stiff equation, Ill-posed equation.

1 Introduction

There are a large number of problems in engineering and science that can be depicted by the nonlinear ordinary differential equations (ODEs) involving some parameters. Particular interest is the solution behavior of the physical problems with one or more of the parameters quite small or quite large. When the boundary conditions are imposed, the resulting problems are usually called the singularly perturbed boundary value problems (SPBVPs). Needless to say, the solutions of SPBVPs have to satisfy the boundary conditions, but for the singular perturbation problems this may be a difficult task, since there is a strong singularity in the boundary layer, which is a thin layer wherein the solution varies rapidly, while away from that layer the solution behaves regularly. Many computational methods have been developed for solving the SPBVPs. For a detailed treatment of the singular perturbation problems one can refer the works by Bender and Orszag (1978), Nayfeh (1981), Kevorkian and Cole (1981, 1996), O'Malley (1991) and De Jager and Jiang (1996). Moreover, for a recent comprehensive survey of the numerical methods for solving the SPBVPs one may refer the review paper by Kadalbajoo and Patidar (2002).

In this paper we will propose new methods for the computations of the following second-order SPBVP:

$$\varepsilon u_1'' + f_1(x,u_1)u_1' + f_2(x,u_1) = 0, \quad 0 < x < 1, \tag{1}$$

$$u_1(0) = \alpha, \quad u_1(1) = \beta, \tag{2}$$

where ε is a small parameter, $f_1(x,u_1)$ and $f_2(x,u_1)$ are given functions, and $[0,1]$ is a spatial range of our problem. The prime denotes the differential with respect to x. For the problems not with the above range, a suitable rescale of the spatial coordinate may bring them into the standard one with a range of $[0,1]$.

We can transform Eqs. (1) and (2) into a mathematical equivalent system:

$$u_1' = u_2, \tag{3}$$

$$u_2' = -\frac{1}{\varepsilon}[f_1(x,u_1)u_2 + f_2(x,u_1)], \tag{4}$$

$$u_1(0) = \alpha, \quad u_1(1) = \beta. \tag{5}$$

[1] Department of Mechanical and Mechatronic Engineering, Taiwan Ocean University, Keelung, Taiwan. E-mail: csliu@mail.ntou.edu.tw

In order to distinguish it from the systems to be introduced later we call Eqs. (3)-(5) the $(\mathbf{u},x)$-BVP, where $\mathbf{u}(x)=(u_1(x),u_2(x))$ denotes the system dependent variables in the x-domain.

For the singular perturbation problems there had already developed many asymptotic approximation methods, and the numerical methods according to these concepts to match the boundary layer behavior were developed in an attempt to obtain the accurate reliable schemes which are uniformly valid with respect to the perturbation parameter [Roos, Stynes and Tobiska (1996)]. Roberts (1982) has introduced a non-asymptotic boundary value method to solve a certain class of singular perturbation problems.

The concept of replacing the SPBVP by an initial value problem (IVP) is presented by Kadalbajoo and Reddy (1987) for a particular type ODE. The original second-order ODE is replaced by an asymptotically equivalent first-order ODEs and is solved as an IVP. Gasparo and Macconi (1989, 1990) gave an initial-value method for the second-order SPBVPs with a boundary layer at one end-point. The idea is to replace the SPBVP by two suitable IVPs, where the two ODEs are integrating on the opposite directions, and the first problem can be solved only if the solution of the second one is known. Then, the initial-value technique developed by Gasparo and Macconi (1989) for solving the singularly-perturbed nonturning-point problems was used by Natesan and Ramanujam (1998) to solve the singularly-perturbed turning-point problems exhibiting twin boundary layers. They obtained the required approximate solution by combining solutions of the reduced problem, an initial-value problem and a terminal-value problem.

A continuance of the IVP technique was developed by Reddy and Chakravthy (2004) and Li and Wang (2005). The given problem is replaced by three first-order ODEs. The numerical solution of two IVPs goes in the positive direction and the third IVP is independent of these two IVPs, integrating on an opposite direction under a specified terminal condition. This technique is mainly limited to the linear SPBVPs.

For the BVPs there are many computational methods by employing the shooting technique [Kubicek and Hlavacek (1983); Keller (1992); Ascher, Mattheij and Russell (1995)]. The shooting method involves a choice of the missing initial condition for Eq. (4), such that the numerical solution at the other end-point can satisfy the constraint $u_1(1)=\beta$ in Eq. (5). If this objective can be achieved very well then one can convert the $(\mathbf{u},x)$-BVP into the $(\mathbf{u},x)$-IVP. Solving the resultant IVP and matching the boundary condition at the other end-point is then the main issue of the shooting method. Frequently, the solution will not immediately satisfy the boundary condition, and, it requires many iterations to feedback the information of mismatch on the target defined by the boundary conditions to adjust the initial guess through some techniques. Thus the solution will gradually converge to the desired boundary condition by varying the initial conditions. This iterative approach is called the shooting method.

The above statement seems rather promising of the shooting method. However, this approach is often ineffective and unstable for the SPBVPs due to the presence of rapidly increasing modes which cannot be solved with the use of an initial value solver. Instead of, a widely used shooting technique is the parallel or multiple shooting to remedy the stability problem. As pointed out by Ascher, Mattheij and Russell (1995) these methods are also likely to be ineffective for more singular problems.

The present approach of the SPBVPs is based on Liu's group preserving scheme (GPS) developed by Liu (2001) for the integration of IVPs. The GPS method is very effective to deal with ODEs endowing with special structures as shown by Liu (2005, 2006a) for stiff equations and for ODEs with constraints. Recently, Liu (2006b) has extended this technique to solve the BVPs, and the numerical results reveal that the GPS is a rather promising method to effectively calculate the two-point BVPs. However, it is not yet been applied to the solutions of SPBVPs.

Before the application of the method developed by Liu (2006b) for the SPBVPs, we will search a one-to-one coordinate transformation, which is designed to smooth out the region where a thin layer appears, featuring by a high gradient variation of the dependent variable. In the transformed domain our shooting method together with the Runge-Kutta method can yield an accurate solution as that for the initial value solver by using a reasonable stepsize. It will be clear that the new method can be applied to the second-order SPBVPs, since we are able to search the missing initial condition through a few trials to search a suitable r in a compact space of $r\in(0,1)$, where the factor r is used in a generalized mid-point rule for the Lie group element of the one-step GPS.

The one-step GPS method for the BVPs has been

named by Liu (2006b) the Lie-group shooting method (LGSM). Liu (2006c, 2006d) has used this concept to develop the numerical estimation method for the unknown temperature-dependent heat conductivity and heat capacity of one-dimensional heat conduction equation. On the other hand, in order to effectively solve the backward in time problems of parabolic PDEs, a past cone structure and a backward group preserving scheme have been successfully developed by the author, such that the new one-step Lie-group numerical methods have been used to solve the backward in time Burgers equation by Liu (2006e), and the backward in time heat conduction equation by Liu, Chang and Chang (2006). Because the Lie-group method possesses a certain advantage than other numerical methods due to its group structure, the Lie-group shooting method is believed to be a powerful technique to solve the SPBVPs.

This paper is arranged as follows. In Section 2 we introduce a coordinate transformation to reduce the singularity in the new coordinate system and point out the relation between singularity and stiffness. In Section 3 we give a brief sketch of the GPS for ODEs, explain the construction of a one-step GPS by using the closure property of the Lie group, and combine it with the generalized mid-point rule to construct a single-parameter Lie group in terms of a weighting factor r. In Section 4 we derive a new Lie-group shooting method to solve the SPBVPs, where we can search the missing initial condition by solving r in a compact space of $r \in (0,1)$. In Section 5 we introduce two new systems obtained by a translation. In Section 6 we consider a finite difference method together with the nonstandard GPS to solve the SPBVPs. In Section 7 we use some numerical examples to demonstrate the efficiency and accuracy of the new methods. Finally, we draw some conclusions in Section 8.

2 Singularity and stiffness

For the SPBVPs, it is hardly and directly applied the shooting method for the numerical solution, since the slope of solution may be a very large value due to a strong singularity in the boundary layer, within which the solution displays a sharp transition when the singular perturbation parameter ε is much smaller than 1. How to choose a suitable initial condition may thus become a rather difficult task when the guesses are carried out in an infinite range of $-\infty < u_1'(0) = A < \infty$.

When ε is small, we may consider a scalar transformation of the x-coordinate by

$$x = 1 - \frac{\tanh[\lambda(1-t)]}{\tanh\lambda}, \tag{6}$$

or its inverse:

$$t = 1 - \frac{1}{\lambda}\ln\frac{1+(1-x)\tanh\lambda}{1-(1-x)\tanh\lambda}, \tag{7}$$

where λ is a suitably selected parameter to wipe out the sharp transition in the boundary layer. The transformation between x and t is one-to-one and onto, and are also $x(0) = 0$ and $x(1) = 1$.

The above coordinates transformation technique has been used by Liu (2006f) to treat the Burgers equation with a very large Reynolds number. It is a typical example for the singularly perturbed partial differential equations.

Through Eq. (6) we can accumulate much of the grid points in the region where the solution appears a sharp variation, and place a small number of grid points in the region where the solution does not change rapidly in the x-domain, even the grid points are uniformly distributed in the t-domain.

From Eqs. (1) and (7) it follows that

$$\frac{\varepsilon\tanh^2\lambda}{\lambda^2(1-\tanh^2[\lambda(1-t)])^2}\ddot{u}_1 - \frac{2\varepsilon\tanh^2\lambda\tanh[\lambda(1-t)]}{\lambda(1-\tanh^2[\lambda(1-t)])^2}\dot{u}_1 + \frac{\tanh\lambda f_1(t,u_1)}{\lambda(1-\tanh^2[\lambda(1-t)])}\dot{u}_1 + f_2(t,u_1) = 0, \tag{8}$$

of which the boundary conditions in Eq. (2) remain unchanged. For saving notation we use the shorthand of $u(t) = u(x(t))$, and now, a superimposed dot denotes the differential with respect to t.

The stepping techniques developed for IVPs require the initial conditions of both u_1 and $u_2 = \dot{u}_1$ for the second-order ODEs. If the initial value $u_2(0) = A$ is available which together with the given condition $u_1(0) = \alpha$, then we can numerically integrate the following IVP step-by-step in a forward direction from $t = 0$ to $t = 1$:

$$\dot{u}_1 = u_2, \tag{9}$$

$$\dot{u}_2 = f(t,u_1,u_2), \tag{10}$$

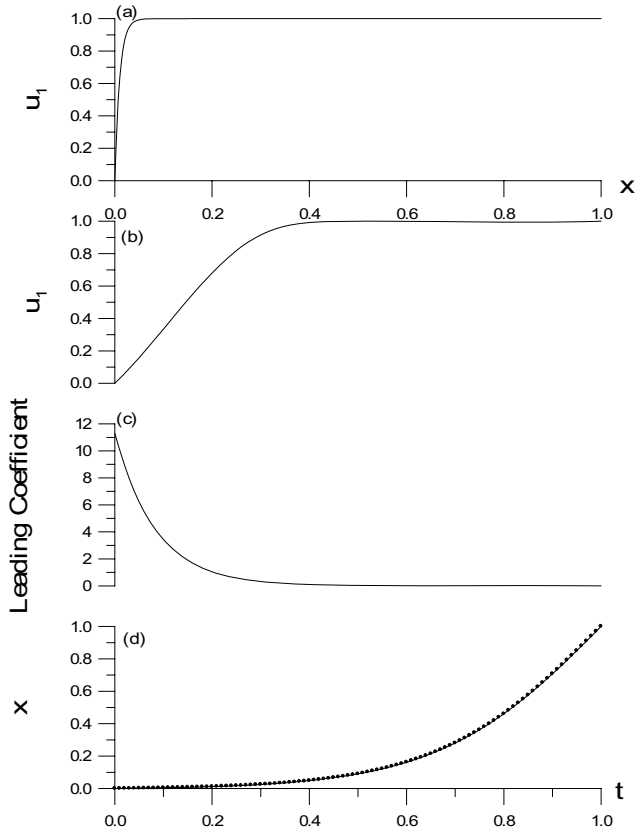

Figure 1 : For Example 1 we plot the exact solution with respect to x in (a), and t in (b). In the t-domain the leading coefficient is plotted in (c), and the relation between x and t is also plotted in (d).

$$u_1(0) = \alpha, \tag{11}$$

$$u_2(0) = A, \tag{12}$$

where

$$f(t,u_1,u_2) := f_3(t,u_1)u_2 + f_4(t,u_1), \tag{13}$$

$$f_3(t,u_1) := 2\lambda\tanh[\lambda(1-t)] - \frac{\lambda(1-\tanh^2[\lambda(1-t)])}{\varepsilon\tanh\lambda} f_1(t,u_1), \tag{14}$$

$$f_4(t,u_1) := -\frac{\lambda^2(1-\tanh^2[\lambda(1-t)])^2}{\varepsilon\tanh^2\lambda} f_2(t,u_1). \tag{15}$$

Here, we call Eqs. (9)-(12) the $(\mathbf{u},t)$-IVP, where $\mathbf{u}(t) = (u_1(t),u_2(t))$ denotes the system variables in the t-domain.

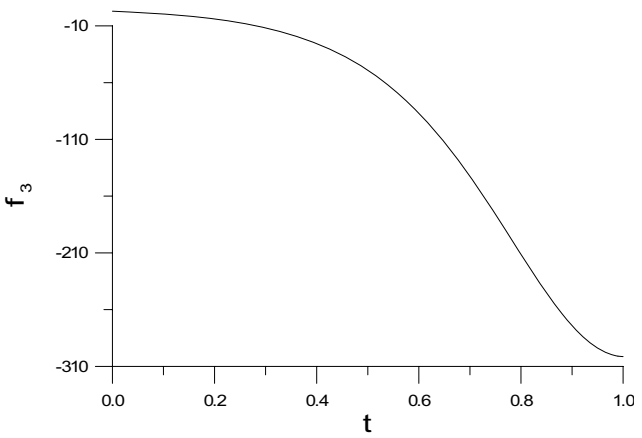

Figure 2 : For Example 1 we plot the function f_3 with respect to t.

To demonstrate the effect of the coordinate transformation in Eq. (6), let us first consider a simple example:

$$\varepsilon u_1'' + u_1' = 0, \;\; u_1(0) = 0, \;\; u_1(1) = 1 \tag{16}$$

with the exact solution given by

$$u_1(x) = \frac{1-\exp(-x/\varepsilon)}{1-\exp(-1/\varepsilon)}. \tag{17}$$

In the plane (x,u_1) as shown in Fig. 1(a) the above solution appears a boundary layer at the left-end point $x = 0$ when $\varepsilon = 0.01$. Through the coordinate transformation in Eq. (7) with $\lambda = 3$, the same curve is plotted in the plane (t,u_1) as shown in Fig. 1(b). It can be seen that the boundary layer becomes width towards to the right-end side, such that the curve is seen more smoothing than that seen in the plane (x,u_1). In Eq. (16) the second order derivative term is multiplied by a small parameter ε, but when Eq. (16) is represented in the form of Eq. (8) with $f_1 = 1$ and $f_2 = 0$ the multiplier before $\ddot{u}_1$ becomes a function of t, the value of which, named the leading coefficient, is plotted in Fig. 1(c). It can be seen that in the transition layer the leading coefficient is finite, no more a small quantity. From Fig. 1(d) it can be seen that there are much grid points accumulated in the thin layer near the end $x = 0$, where the grid points are uniformly distributed in the t-axis.

Now, we can check Eq. (16) in the form of Eqs. (9) and (10) by substituting $f_1 = 1$ and $f_2 = 0$ into Eqs. (14) and (15). Under the same parameters of $\varepsilon = 0.01$ and $\lambda = 3$, we plot the coefficient function f_3 before the variable u_2

in Fig. 2. When compared with the coefficient before u_2 in Eq. (9), it can be seen that the absolute value of f_3 is much larger than 1, especially when t increases.

According to the definition made by Shampine and Gear (1979), the initial value problem (9)-(12) is said to be stiff, if at every point $(\mathbf{u},t)$ of the solution curve the system matrix has at least one eigenvalue whose real part is large negative, whilst the real part of other eigenvalue does not take large positive value. When expressed Eq. (16) as the system of Eqs. (9) and (10) in the t-domain, Fig. 2 shows the negative eigenvalue may large up to -300 while the other one is 0, which indicates that the new system exhibits certain stiffness. For comparison let us mention that Eq. (16) itself is also a stiff BVP, of which the two eigenvalues are 0 and $-1/\varepsilon = -100$ when $\varepsilon = 0.01$. Of course, it is not so stiff as the new system of Eqs. (9) and (10) in the t-domain.

Through the above explanation it reveals that the singularity of the original problem in the x-domain renders the stiffness of the new system of Eqs. (9) and (10) in the t-domain. The stiffness grows with t. Therefore, in the development of the new method we should take the effect of stiffness into account on the numerical integration of the IVP in Eqs. (9)-(12).

When we choose $\lambda = 0.1$ it reveals that the effect of coordinate transformation disappears since it is almost $x = t$. The coordinate transformation parameter λ plays a role to reduce the singularity of the original SPBVP in the x-domain; however, it also increases the stiffness of the new system of Eqs. (9) and (10) in the t-domain. In a practical computation of the SPBVPs by employing the shooting method, it is rather crucial to select a suitable λ, which is a trade-off between the singularity-free and stiffness. More large λ is, more singularity can be depressed, and however, the resultant new system is more stiff. In any way, for a highly singular problem the new system of Eqs. (9) and (10) in the t-domain is more possibly to allow us to develop an effective shooting technique rather than that of the original equations (3) and (4) in the x-domain.

In the next two sections we are going to develop the shooting method basing on the author's Lie group mapping technique, which is shown to be very effective for the second-order BVP [Liu (2006b)]. For a self-content reason we have to repeat some previous results but only showing a brief sketch of the mathematical methods.

3 One-step GPS

3.1 The GPS

The above discussions prompt us to integrate Eqs. (9) and (10) in the t-domain rather than that to integrate Eqs. (3) and (4) in the x-domain. For this purpose let us write Eqs. (9) and (10) in the vector form:

$$\dot{\mathbf{u}} = \mathbf{f}(t,\mathbf{u}), \tag{18}$$

where

$$\mathbf{u} := \begin{bmatrix} u_1 \\ u_2 \end{bmatrix}, \quad \mathbf{f} := \begin{bmatrix} u_2 \\ f(t,u_1,u_2) \end{bmatrix}. \tag{19}$$

Liu (2001) has embedded Eq. (18) into an augmented system:

$$\dot{\mathbf{X}} := \frac{d}{dt}\begin{bmatrix} \mathbf{u} \\ \|\mathbf{u}\| \end{bmatrix} = \begin{bmatrix} \mathbf{0}_{2\times 2} & \frac{\mathbf{f}(t,\mathbf{u})}{\|\mathbf{u}\|} \\ \frac{\mathbf{f}^{\mathrm{T}}(t,\mathbf{u})}{\|\mathbf{u}\|} & 0 \end{bmatrix} \begin{bmatrix} \mathbf{u} \\ \|\mathbf{u}\| \end{bmatrix} := \mathbf{A}\mathbf{X}, \tag{20}$$

where $\mathbf{A}$ is an element of the Lie algebra $so(2,1)$ satisfying

$$\mathbf{A}^{\mathrm{T}}\mathbf{g} + \mathbf{g}\mathbf{A} = \mathbf{0} \tag{21}$$

with

$$\mathbf{g} = \begin{bmatrix} \mathbf{I}_2 & \mathbf{0}_{2\times 1} \\ \mathbf{0}_{1\times 2} & -1 \end{bmatrix} \tag{22}$$

a Minkowski metric. Here, $\mathbf{I}_2$ is the identity matrix, and the superscript T stands for the transpose.

The augmented variable $\mathbf{X}$ satisfies the cone condition:

$$\mathbf{X}^{\mathrm{T}}\mathbf{g}\mathbf{X} = \mathbf{u}\cdot\mathbf{u} - \|\mathbf{u}\|^2 = 0. \tag{23}$$

Accordingly, Liu (2001) has developed a group-preserving scheme (GPS) given as follows:

$$\mathbf{X}_{k+1} = \mathbf{G}(k)\mathbf{X}_k, \tag{24}$$

where $\mathbf{X}_k$ denotes the numerical value of $\mathbf{X}$ at the discrete t_k, and $\mathbf{G}(k) \in SO_o(2,1)$ satisfies

$$\mathbf{G}^{\mathrm{T}}\mathbf{g}\mathbf{G} = \mathbf{g}, \tag{25}$$

$$\det \mathbf{G} = 1, \tag{26}$$

$$G_0^0 > 0, \tag{27}$$

where G_0^0 is the 00th component of $\mathbf{G}$.

3.2 Generalized mid-point rule

Applying the scheme (24) to Eq. (20) with a specified initial condition $\mathbf{X}(0)=\mathbf{X}_0$ we can compute the solution $\mathbf{X}(t)$ by GPS. Assuming that the stepsize used in GPS is $h=1/K$, and starting from an initial augmented condition $\mathbf{X}_0=\mathbf{X}(0)=(\mathbf{u}_0^{\mathrm{T}},\|\mathbf{u}_0\|)^{\mathrm{T}}$ we want to calculate the value $\mathbf{X}(1)=(\mathbf{u}^{\mathrm{T}}(1),\|\mathbf{u}(1)\|)^{\mathrm{T}}$ at $t=1$.

By applying Eq. (24) step-by-step we can obtain

$$\mathbf{X}_f=\mathbf{G}_K(h)\cdots\mathbf{G}_1(h)\mathbf{X}_0, \tag{28}$$

where $\mathbf{X}_f$ may approximate the exact $\mathbf{X}(1)$ with a certain accuracy. However, let us recall that each $\mathbf{G}_i$, $i=1,\ldots,K$, is an element of the Lie group $SO_o(2,1)$, and by the closure property of the Lie group, $\mathbf{G}_K(h)\cdots\mathbf{G}_1(h)$ is also a Lie group denoted by $\mathbf{G}$. Hence, we have

$$\mathbf{X}_f=\mathbf{G}\mathbf{X}_0. \tag{29}$$

This is a one-step transformation from $\mathbf{X}_0$ to $\mathbf{X}_f$.

We can calculate $\mathbf{G}$ by a generalized mid-point rule, which is obtained from an exponential mapping of $\mathbf{A}$ by taking the values of the argument variables of $\mathbf{A}$ at a generalized mid-point. The Lie group generated from $\mathbf{A}\in so(2,1)$ is known as a proper orthochronous Lorentz group, which admits a closed-form representation given as follows:

$$\mathbf{G}=\begin{bmatrix}\mathbf{I}_2+\frac{(a-1)}{\|\hat{\mathbf{f}}\|^2}\hat{\mathbf{f}}\hat{\mathbf{f}}^{\mathrm{T}} & \frac{b\hat{\mathbf{f}}}{\|\hat{\mathbf{f}}\|}\\ \frac{b\hat{\mathbf{f}}^{\mathrm{T}}}{\|\hat{\mathbf{f}}\|} & a\end{bmatrix}, \tag{30}$$

where

$$\hat{\mathbf{u}}=r\mathbf{u}_0+(1-r)\mathbf{u}_f, \tag{31}$$

$$\hat{\mathbf{f}}=\mathbf{f}(\hat{t},\hat{\mathbf{u}}), \tag{32}$$

$$a=\cosh\left(\frac{\|\hat{\mathbf{f}}\|}{\|\hat{\mathbf{u}}\|}\right), \tag{33}$$

$$b=\sinh\left(\frac{\|\hat{\mathbf{f}}\|}{\|\hat{\mathbf{u}}\|}\right). \tag{34}$$

Here, we use the initial $\mathbf{u}_0$ and the final $\mathbf{u}_f$ through a suitable weighting factor r to calculate $\mathbf{G}$, where $0<r<1$ is a parameter and $\hat{t}=r$. The above method applied a generalized mid-point rule on the calculation of $\mathbf{G}$, and the resultant is a single-parameter Lie group element denoted by $\mathbf{G}(r)$.

3.3 A Lie group mapping between two points on the cone

Let us define a new vector

$$\mathbf{F}:=\frac{\hat{\mathbf{f}}}{\|\hat{\mathbf{u}}\|}, \tag{35}$$

such that Eqs. (30), (33) and (34) can be also expressed as

$$\mathbf{G}=\begin{bmatrix}\mathbf{I}_2+\frac{a-1}{\|\mathbf{F}\|^2}\mathbf{F}\mathbf{F}^{\mathrm{T}} & \frac{b\mathbf{F}}{\|\mathbf{F}\|}\\ \frac{b\mathbf{F}^{\mathrm{T}}}{\|\mathbf{F}\|} & a\end{bmatrix}, \tag{36}$$

$$a=\cosh(\|\mathbf{F}\|), \tag{37}$$

$$b=\sinh(\|\mathbf{F}\|). \tag{38}$$

From Eqs. (29) and (36) it follows that

$$\mathbf{u}_f=\mathbf{u}_0+\eta\mathbf{F}, \tag{39}$$

$$\|\mathbf{u}_f\|=a\|\mathbf{u}_0\|+b\frac{\mathbf{F}\cdot\mathbf{u}_0}{\|\mathbf{F}\|}, \tag{40}$$

where

$$\eta:=\frac{(a-1)\mathbf{F}\cdot\mathbf{u}_0+b\|\mathbf{u}_0\|\|\mathbf{F}\|}{\|\mathbf{F}\|^2}. \tag{41}$$

Substituting

$$\mathbf{F}=\frac{1}{\eta}(\mathbf{u}_f-\mathbf{u}_0) \tag{42}$$

into Eq. (40) we obtain

$$\frac{\|\mathbf{u}_f\|}{\|\mathbf{u}_0\|}=a+b\frac{(\mathbf{u}_f-\mathbf{u}_0)\cdot\mathbf{u}_0}{\|\mathbf{u}_f-\mathbf{u}_0\|\|\mathbf{u}_0\|}, \tag{43}$$

where

$$a=\cosh\left(\frac{\|\mathbf{u}_f-\mathbf{u}_0\|}{\eta}\right), \tag{44}$$

$$b = \sinh\left(\frac{\|\mathbf{u}_f - \mathbf{u}_0\|}{\eta}\right) \tag{45}$$

are obtained by inserting Eq. (42) for $\mathbf{F}$ into Eqs. (37) and (38).

Let

$$\cos\theta := \frac{[\mathbf{u}_f - \mathbf{u}_0]\cdot\mathbf{u}_0}{\|\mathbf{u}_f - \mathbf{u}_0\|\|\mathbf{u}_0\|}, \tag{46}$$

$$S := \|\mathbf{u}_f - \mathbf{u}_0\|, \tag{47}$$

and from Eqs. (43)-(45) it follows that

$$\frac{\|\mathbf{u}_f\|}{\|\mathbf{u}_0\|} = \cosh\left(\frac{S}{\eta}\right) + \cos\theta\sinh\left(\frac{S}{\eta}\right). \tag{48}$$

By defining

$$Z := \exp\left(\frac{S}{\eta}\right), \tag{49}$$

we obtain a quadratic equation for Z from Eq. (48):

$$(1+\cos\theta)Z^2 - \frac{2\|\mathbf{u}_f\|}{\|\mathbf{u}_0\|}Z + 1 - \cos\theta = 0. \tag{50}$$

The solution is found to be

$$Z = \frac{\frac{\|\mathbf{u}_f\|}{\|\mathbf{u}_0\|} + \sqrt{\left(\frac{\|\mathbf{u}_f\|}{\|\mathbf{u}_0\|}\right)^2 - 1 + \cos^2\theta}}{1+\cos\theta}, \tag{51}$$

and then from Eqs. (49) and (47) we obtain

$$\eta = \frac{\|\mathbf{u}_f - \mathbf{u}_0\|}{\ln Z}. \tag{52}$$

Therefore, between any two points $(\mathbf{u}_0, \|\mathbf{u}_0\|)$ and $(\mathbf{u}_f, \|\mathbf{u}_f\|)$ on the cone, there exists a Lie group element $\mathbf{G} \in SO_o(2,1)$ mapping $(\mathbf{u}_0, \|\mathbf{u}_0\|)$ onto $(\mathbf{u}_f, \|\mathbf{u}_f\|)$, which is given by

$$\begin{bmatrix} \mathbf{u}_f \\ \|\mathbf{u}_f\| \end{bmatrix} = \mathbf{G}\begin{bmatrix} \mathbf{u}_0 \\ \|\mathbf{u}_0\| \end{bmatrix}, \tag{53}$$

where $\mathbf{G}$ is uniquely determined by $\mathbf{u}_0$ and $\mathbf{u}_f$ through the following equations:

$$\mathbf{G} = \begin{bmatrix} \mathbf{I}_2 + \frac{a-1}{\|\mathbf{F}\|^2}\mathbf{F}\mathbf{F}^{\mathrm{T}} & \frac{b\mathbf{F}}{\|\mathbf{F}\|} \\ \frac{b\mathbf{F}^{\mathrm{T}}}{\|\mathbf{F}\|} & a \end{bmatrix}, \tag{54}$$

$$a = \cosh(\|\mathbf{F}\|), \tag{55}$$

$$b = \sinh(\|\mathbf{F}\|), \tag{56}$$

$$\mathbf{F} = \frac{1}{\eta}(\mathbf{u}_f - \mathbf{u}_0), \tag{57}$$

in which η is still calculated by Eq. (52).

4 The Lie-group shooting method for SPBVP

The SPBVPs considered in Section 1 require information at the initial point $t = 0$ and a terminal point $t = 1$. However, the usual stepping scheme requires a complete information at the starting point $t = 0$. Some effort is still required to adjust the stepping scheme for the integration of the SPBVPs presented there.

From Eqs. (9)-(12) it follows that

$$\dot{u}_1 = u_2, \tag{58}$$

$$\dot{u}_2 = f(t, u_1, u_2), \tag{59}$$

$$u_1(0) = \alpha, \;\; u_1(1) = \beta, \tag{60}$$

$$u_2(0) = A, \;\; u_2(1) = B, \tag{61}$$

where A and B are two supplemented unknown constants, and α and β are two given constants from the specified boundary conditions.

From Eqs. (39), (60) and (61) it follows that

$$\mathbf{F} := \begin{bmatrix} F_1 \\ F_2 \end{bmatrix} = \frac{1}{\eta}\begin{bmatrix} \beta - \alpha \\ B - A \end{bmatrix}. \tag{62}$$

Starting from an initial guess of (A, B) we use the following equation to calculate η:

$$\eta = \frac{\sqrt{(\alpha-\beta)^2 + (A-B)^2}}{\ln Z}, \tag{63}$$

in which Z is calculated by

$$Z = \frac{\frac{\sqrt{\beta^2+B^2}}{\sqrt{\alpha^2+A^2}} + \sqrt{\frac{\beta^2+B^2}{\alpha^2+A^2} - (1-\cos^2\theta)}}{1+\cos\theta}, \tag{64}$$

where

$$\cos\theta = \frac{\alpha(\beta-\alpha)+A(B-A)}{\sqrt{(\alpha-\beta)^2+(A-B)^2}\sqrt{\alpha^2+A^2}}. \tag{65}$$

The above three equations are obtained from Eqs. (52), (51) and (46) by inserting Eq. (19) for **u**.

When comparing Eq. (62) with Eq. (35), and with the aid of Eqs. (31), (32) and (58)-(61) we obtain

$$A = \frac{1}{\eta\xi}[\xi^2(\beta-\alpha)-(1-r)\eta^2\hat{f}], \tag{66}$$

$$B = \frac{1}{\eta\xi}[\xi^2(\beta-\alpha)+r\eta^2\hat{f}], \tag{67}$$

where

$$\hat{f} := f(r, r\alpha+(1-r)\beta, rA+(1-r)B), \tag{68}$$

$$\xi := \sqrt{[r\alpha+(1-r)\beta]^2+[rA+(1-r)B]^2}. \tag{69}$$

The above derivation of the governing equations (63)-(69) is based on that by equating the two **F**'s in Eqs. (35) and (57). It also means that the two Lie groups defined by Eqs. (30) and (54) are equal. Under this sense we may call our shooting technique a Lie-group shooting method.

Inserting Eq. (13) for $\hat{f}$ into Eqs. (66) and (67) we can rearrange them into a neater form:

$$A = \frac{\xi}{\eta}(\beta-\alpha)-(1-r)(\beta-\alpha)\hat{f}_3-\frac{(1-r)\eta}{\xi}\hat{f}_4, \tag{70}$$

$$B = \frac{\xi}{\eta}(\beta-\alpha)+r(\beta-\alpha)\hat{f}_3+\frac{r\eta}{\xi}\hat{f}_4, \tag{71}$$

where

$$\hat{f}_3 = 2\lambda\tanh[\lambda(1-r)] - \frac{\lambda(1-\tanh^2[\lambda(1-r)])}{\varepsilon\tanh\lambda}f_1(r, r\alpha+(1-r)\beta), \tag{72}$$

$$\hat{f}_4 = -\frac{\lambda^2(1-\tanh^2[\lambda(1-r)])^2}{\varepsilon\tanh^2\lambda}f_2(r, r\alpha+(1-r)\beta). \tag{73}$$

For a specified r and the given functions f_1 and f_2, Eqs. (70) and (71) can be used to generate a new (A,B) by repeating the above process until (A,B) converges according to a given stopping criterion:

$$\sqrt{(A_{i+1}-A_i)^2+(B_{i+1}-B_i)^2} \le \varepsilon_1. \tag{74}$$

If A is available, we can return to integrate Eqs. (9)-(12) by a suitable forward IVP solver.

So far, we have not yet said that how to determine r. For a trial r, let $u_1^r(1)$ denote the corresponding solution of u_1 at $t=1$. We start from $r=1/2$ to determine A by Eqs. (63)-(74), then numerically integrate Eqs. (9)-(12) from $t=0$ to $t=1$, and compare the end value of $u_1(1)$ with the exact β. If $|u_1^{1/2}(1)-\beta|$ is smaller than a given tolerance error ε_2, then the process of finding solution is finished. Otherwise, we need to calculate the values of $u_1(1)$ corresponding to a different $r_1<0.5$ or $r_2>0.5$, which are denoted by $u_1^{r_1}(1)$ and $u_1^{r_2}(1)$, respectively. If $[u_1^{r_1}(1)-\beta][u_1^{1/2}(1)-\beta]<0$, then there exists one root of r between r_1 and 0.5, which renders $u_1^r(1)-\beta=0$; otherwise, the root is located between $(0.5, r_2)$. Then, we apply the half-interval method to find a suitable r, which requires us to calculate Eqs. (9)-(12) at each of the calculation of $u_1^r(1)-\beta$, until $|u_1^r(1)-\beta|$ is small enough to satisfy the criterion of $|u_1^r(1)-\beta|\le\varepsilon_2$, where ε_2 is a given error tolerance.

5 The translation to new systems

For the singularly perturbed equation, the slope of u_1, i.e., u_2, may be large at one or both of the two ends of the interval, which thus makes A or/and B rather large. Under these conditions the $\cos\theta$ defined in Eq. (65) may be approaching -1, which renders Eq. (64) not applicable in the estimation of A and B, because they are much larger than α and β. In order to increase the stability of our shooting method, we can consider a translation of u_1 by $y_1=u_1+c$, where c is a constant.

Therefore we can obtain a new system:

$$y_1' = y_2, \tag{75}$$

$$y_2' = -\frac{1}{\varepsilon}[f_1(x, y_1-c)y_2+f_2(x, y_1-c)], \tag{76}$$

$$y_1(0)=\alpha+c, \quad y_1(1)=\beta+c. \tag{77}$$

This system will be called the $(\mathbf{y},x)$-BVP, where $\mathbf{y}(x) = (y_1(x), y_2(x))$ denotes the system variables in the x-domain. Similarly, we may apply the shooting method in Section 4 to this system for finding a missing initial condition $y_2(0) = A_x$. If A_x is available, we can change the $(\mathbf{y},x)$-BVP to the $(\mathbf{y},x)$-IVP.

By applying the coordinate transformation in Eq. (4), we can obtain the following $(\mathbf{y},t)$-IVP, which is supplemented with an unknown initial condition $y_2(0) = A$:

$$\dot{y}_1 = y_2, \tag{78}$$

$$\dot{y}_2 = f(t, y_1 - c, y_2), \tag{79}$$

$$y_1(0) = \alpha + c, \tag{80}$$

$$y_2(0) = A, \tag{81}$$

where

$$A = \frac{\lambda(1-\tanh^2\lambda)}{\tanh\lambda} A_x. \tag{82}$$

We can apply the fourth-order Runge-Kutta method (RK4) to integrate the above $(\mathbf{y},x)$-IVP or the $(\mathbf{y},t)$-IVP system by the following formula:

$$\mathbf{y}_{n+1} = \mathbf{y}_n + \frac{h}{6}[\mathbf{f}_1 + 2\mathbf{f}_2 + 2\mathbf{f}_3 + \mathbf{f}_4], \tag{83}$$

where

$$\mathbf{f}_1 = \mathbf{f}(t_n, \mathbf{y}_n), \tag{84}$$

$$\mathbf{f}_2 = \mathbf{f}(t_n + \tau, \mathbf{y}_n + \tau\mathbf{f}_1), \tag{85}$$

$$\mathbf{f}_3 = \mathbf{f}(t_n + \tau, \mathbf{y}_n + \tau\mathbf{f}_2), \tag{86}$$

$$\mathbf{f}_4 = \mathbf{f}(t_n + h, \mathbf{y}_n + h\mathbf{f}_3), \tag{87}$$

in which $\tau = h/2$ is one half of the stepsize.

6 Singularity and ill-posedness

We have mentioned that when ε is very small, the resultant $(\mathbf{u},t)$-IVP or the $(\mathbf{y},t)$-IVP obtained through a translation is very stiff. Usually, it is hardly applied the RK4 method to integrate the resulting stiff equations unless the stepsize is taken to be very small for a stable integration. In order to provide an alternative way to solve such SPBVPs with a reasonable grid size we may consider a finite difference method as follows.

6.1 Finite difference

Here we consider a finite difference of Eq. (1) with u_1 replaced by u:

$$u_{i+1} - 2u_i + u_{i-1} + \frac{\Delta x}{\varepsilon} f_1(x, u_i)[u_{i+1} - u_i] + \frac{(\Delta x)^2}{\varepsilon} f_2(x, u_i) = 0, \tag{88}$$

where $\Delta x = 1/n$ is the spatial length, and $u_i = u(i\Delta x)$, $i = 1, \ldots, n-1$, are unknown values of $u(x)$ at the grid points. However, $u_0 = \alpha$ and $u_n = \beta$ are the given boundary conditions.

Being a new strategy we will consider u_i to be the steady-state solutions of the following differential equations:

$$\dot{u}_i = u_{i+1} - 2u_i + u_{i-1} + \frac{\Delta x}{\varepsilon} f_1(x, u_i)[u_{i+1} - u_i] + \frac{(\Delta x)^2}{\varepsilon} f_2(x, u_i). \tag{89}$$

For a highly singular BVP in Eqs. (1) and (2), the resulting finite difference equation (88) is also highly ill-posed because the Jacobian matrix has a large condition number, which also renders Eq. (89) very stiff.

Usually we require our integration of Eq. (89) to a large extent of t in order to get the steady-state solution. If the stepsize of a numerical scheme is restricted to be small due to a stable reason, it is hardly to be used in the integration of stiff equation (89).

An effective scheme is developed by Liu (2005) by considering the nonstandard difference method for solving the very stiff problems, which basing on the group preserving scheme proposed by Liu (2001) stated as follows for self-content.

6.2 The NGPS

The nonstandard finite difference used here is replacing the Euler approximation of

$$\dot{\mathbf{u}} \approx \frac{\mathbf{u}_{k+1}-\mathbf{u}_k}{h}, \tag{90}$$

by a nonstandard approximation

$$\dot{\mathbf{u}} \approx \frac{\mathbf{u}_{k+1}-\mathbf{u}_k}{\phi(h)}, \tag{91}$$

where $\phi(h)$ is a denominator function with the properties $\phi(h)>0$ and $\phi(h)=h+O(h^2)$.

For the stiff differential equations we may adopt

$$\phi(h)=\frac{1-\exp(-\rho h)}{\rho}, \tag{92}$$

where ρ is a number not smaller than the Lipschitz constant of Eq. (89).

The replacement of h by $\phi(h)$ in Eq. (91) has inspired Liu (2005), according to a Cayley transformation technique, to derive the following stiff integrator:

$$\mathbf{u}_{k+1}=\mathbf{u}_k+\frac{4\|\mathbf{u}_k\|^2+2\phi\mathbf{f}_k\cdot\mathbf{u}_k}{4\|\mathbf{u}_k\|^2-\phi^2\|\mathbf{f}_k\|^2}\phi\mathbf{f}_k, \tag{93}$$

where $\mathbf{u}=(u_1,\ldots,u_{n-1})$.

The combination of nonstandard method with group preserving scheme, namely the nonstandard group preserving scheme (NGPS), renders the new numerical scheme (93) always stable. This result is very important for the stiff differential equations, because the dominant factor to choose a suitable stepsize for the stiff differential equation is its stability, not its accuracy, as demonstrated by Shampine and Gear (1979).

7 Numerical examples

In order to assess the performance of the newly developed methods let us investigate the following examples.

7.1 Example 1

The first example given by Eq. (16) is calculated here again but by the newly developed method in Section 4.

We are going to search a missing initial condition $u_2(0)=A$, such that in the numerical solutions of Eqs. (9)-(12), $u_1(1)$ can match very well the exact value $u_1(1)=1$.

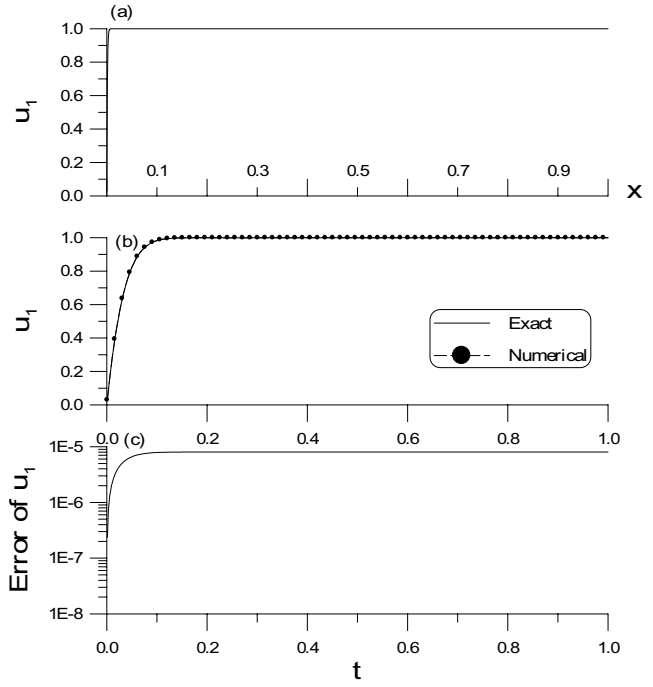

Figure 3 : For Example 1 with $\varepsilon=0.001$: (a) plotting the exact solution with respect to x, (b) comparing with the numerical solution, (c) the numerical error.

We first consider a moderate singularity with $\varepsilon=0.001$. The coordinate tansformation parameter is taken to be $\lambda=3$. The RK4 was used to integrate the resulting $(\mathbf{y},t)$-IVP of Eqs. (78)-(81) with $c=100$ and a stepsize $h=0.001$.

We take $[0.03,0.035]$ to be the range of r. In the estimation of A, the criterion in Eq. (74) with $\varepsilon_1=10^{-10}$ was used. The initial (A,B) is taken to be $(A,B)=(1,-1)$. Then we use a half-interval method to search an accurate r, which is converged through 11 iterations under an error tolerance of $\varepsilon_2=10^{-5}$. The final value of u_1 matches very well with the exact value with an error 7.995×10^{-6}. The relative error of the initial value of u_2 is about 8×10^{-6}. In Fig. 3 we compare the numerical result with the exact solution. It can be seen that the numerical error of u_1 is in the order of 10^{-6}. From Fig. 3(a) it can be seen that in the plane (x,u_1) the solution rapidly increases from 0 to 1. In order to make the comparison clear we plot both the numerical and exact solutions in the plane (t,u_1) as shown in Fig. 3(b). The maximum

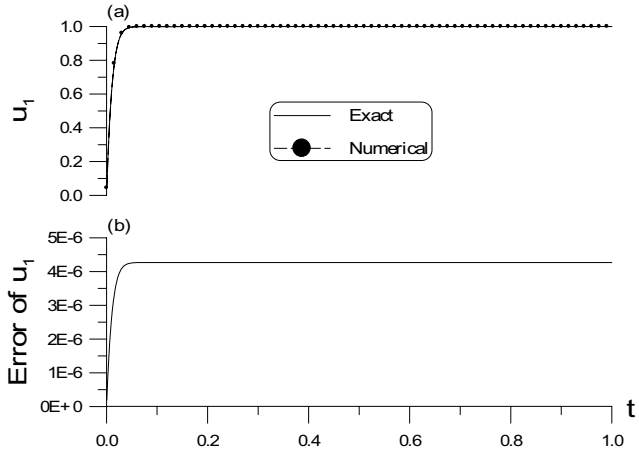

Figure 4 : For Example 1 with $\varepsilon = 0.00001$: (a) comparing the numerical and exact solutions, and (b) the numerical error.

error is 8×10^{-6} as shown in Fig. 3(c).

Next, we consider a strong singularity with $\varepsilon = 0.00001$. The coordinate tansformation parameter is taken to be $\lambda = 5$. The RK4 was used to integrate the resulting $(\mathbf{y},t)$-IVP of Eqs. (78)-(81) with $c = 200$ and a stepsize $h = 0.0001$. We take $[0.01, 0.011]$ to be the range of r. In the estimation of A, the criterion in Eq. (74) with $\varepsilon_1 = 10^{-10}$ was used. The initial (A,B) is taken to be $(A,B) = (1,-1)$. Then we use a half-interval method to search an accurate r, which is converged through 9 iterations under an error tolerance of $\varepsilon_2 = 10^{-5}$. The final value of u_1 matches very well with the exact value with an error 4.268×10^{-6}. The relative error of the initial value of u_2 is about 4.27×10^{-6}. In Fig. 4(a) we compare the numerical result with the exact solution. It can be seen that these two solutions are almost identical, and the numerical error of u_1 is in the order of 10^{-6} as shown in Fig. 4(b). The maximum error is 4.268×10^{-6}. This example reveals that a much smaller singular parameter ε does not deterioiate the accuracy of our numerical solution, if λ is selected suitably and the integration stepsize is slighly decreased.

In principle, we can increase the accuracy by imposing a smaller ε_2 on the shooting error, which however requires more iterations. Since the numerical method is very stable we can quickly pick up the correct value of r through some trials and modifications. Therefore, in the following calculations of other examples we do not use the above half-interval method again to pick up the weighting factor r.

7.2 Example 2

We calculate the second example given by Eq. (16) but adding with a nonhomogeneous term on the right-hand side:

$$\varepsilon u_1'' + u_1' = 1 + 2x, \tag{94}$$

$$u_1(0) = 0, \;\; u_1(1) = 1. \tag{95}$$

This example has been calculated by Varner and Choudhury (1998), and Ilicasu and Schultz (2004) with high-order finite difference methods.

In order to compare our numerical result with that of the above cited papers, we first fix $\varepsilon = 0.01$. The translation constant $c = 50$ is also fixed.

Because of $\varepsilon = 0.01$, the system is not too singular, and we directly apply the shooting method in Section 4 and the RK4 method to the resulting $(\mathbf{y},x)$-IVP. Through some trials we have picked up the parameter r to be $r = 0.6839256912$. When compared the estimated $A_x = -97.019999996$ with the exact one $u_2(0) = -97.02$ calculated from the closed-form solution:

$$u_1(x) = x(x+1-2\varepsilon) + (2\varepsilon - 1)\frac{1-\exp(-x/\varepsilon)}{1-\exp(-1/\varepsilon)}, \tag{96}$$

the error is very small with 4.258×10^{-9}. At the same time, the final value of u_1 matches very well with the exact value with an error 4.252×10^{-11}.

By using the above estimated initial condition of $u_2(0) = A_x$ and the given $u_1(0) = 0$, we can integrate the $(\mathbf{y},x)$-IVP by the RK4 method with a $\Delta x = 0.0005$, which is the same as that used by Varner and Choudhury (1998) and Ilicasu and Schultz (2004). In Fig. 5(a) we plot the numerical and exact solutions, which are almost coincident. Thus, we plot the numerical error in Fig. 5(b), which are obtained by taking the absolute of the differences between numerical and exact solutions. In Table 1 we also list the numerical errors of the numerical results obtained by Varner and Choudhury (1998). Obviously, our errors are much smaller than that of Varner and Choudhury (1998).

Ilicasu and Schultz (2004) have calculated this case by using the high-order finite-difference method. Our maximum error is 1.96×10^{-8}, which is slightly larger than

Table 1 : For Example 2 we comparing the numerical errors under $\varepsilon = 0.01$ and at different x with that of Varner and Choudhury (1998) denoted as VC.

x	VC	$(\mathbf{y},x)$	$(\mathbf{y},t)$
0.002	3.6×10^{-5}	8.7×10^{-9}	2.1×10^{-10}
0.004	5.0×10^{-5}	1.4×10^{-7}	4.1×10^{-10}
0.006	7.3×10^{-5}	1.8×10^{-7}	5.7×10^{-10}
0.008	8.1×10^{-5}	1.9×10^{-7}	7.1×10^{-10}
0.010	8.4×10^{-5}	2.0×10^{-7}	8.4×10^{-10}
0.012	8.4×10^{-5}	1.9×10^{-7}	9.3×10^{-10}
0.014	8.1×10^{-5}	1.8×10^{-7}	1.0×10^{-9}
0.016	7.8×10^{-5}	1.7×10^{-7}	1.1×10^{-9}
0.018	7.3×10^{-5}	1.6×10^{-7}	1.1×10^{-9}
0.020	6.9×10^{-5}	1.4×10^{-7}	1.2×10^{-9}
0.022	6.3×10^{-5}	1.3×10^{-7}	1.2×10^{-9}
0.024	6.0×10^{-5}	1.2×10^{-7}	1.2×10^{-9}
0.026	4.4×10^{-5}	1.0×10^{-7}	1.2×10^{-9}
0.028	5.0×10^{-5}	9.1×10^{-8}	1.2×10^{-9}
0.030	4.6×10^{-5}	8.0×10^{-8}	1.2×10^{-9}

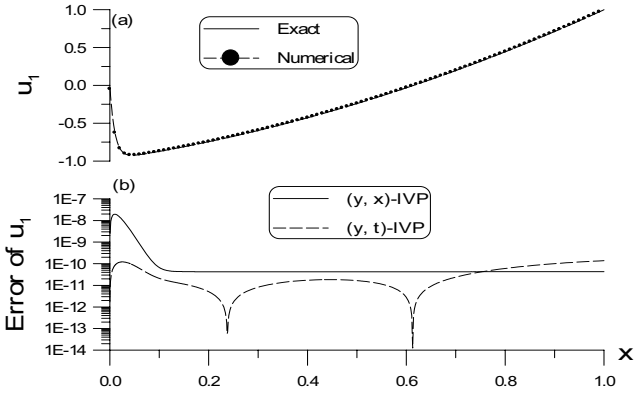

Figure 5 : For Example 2 with $\varepsilon = 0.01$: (a) comparing the numerical and exact solutions, and (b) the numerical errors.

that of 0.63×10^{-8} obtained by Ilicasu and Schultz (2004).

The resulting $(\mathbf{y},x)$-IVP is indeed a singular system and when apply the RK4 to it the accuracy is constrained to a certain degree. Instead of, we apply the RK4 to the resulting $(\mathbf{y},t)$-IVP through a coordinate transformation with $\lambda = 2$. The initial values are obtained from Eqs. (80)-(82) by inserting the above estimated A_x, $\alpha = 0$, $\lambda = 2$ and $c = 50$. Under a larger stepsize with $h = 0.001$ as compared with the above $\Delta x = 0.0005$ we obtain very

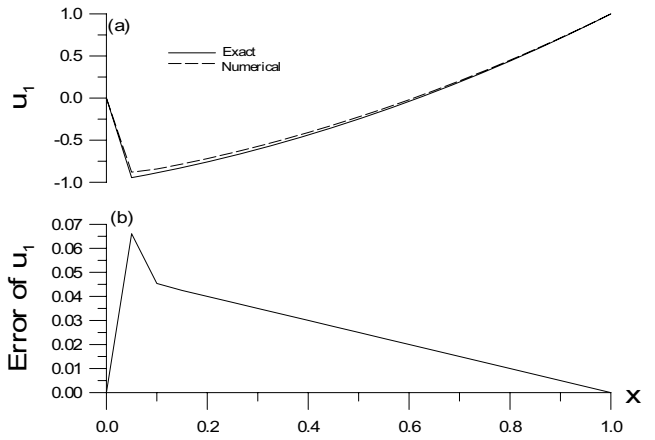

Figure 6 : For Example 2 with $\varepsilon = 0.001$ solved by the NGPS: (a) comparing the numerical and exact solutions, and (b) the numerical error.

accurate results, whose numerical error is shown in Table 1 and is also plotted in Fig. 5(b) for a comparison. Under the same stepsize, Ilicasu and Schultz (2004) obtained the numerical solutions with the maximum error 10^{-7}, which is much larger than our maximum error 1.3746×10^{-10}.

Next we consider two cases of $\varepsilon = 10^{-3}$ and $\varepsilon = 10^{-4}$, and apply the NGPS method in Section 6.2 to integrate Eq. (89) of this example with the following parameters: $\Delta x = 1/20$ (i.e. $n = 20$), $\rho = 50$, $h = 1$. After 36 iterations the steady-state solution is obtained by subjecting to $\|\mathbf{u}_{k+1} - \mathbf{u}_k\| < \varepsilon_2$, where $\mathbf{u}_k$ denotes the k-th iterative value of $\mathbf{u} = (u_1, \ldots, u_{n-1})$. For this case we use $\varepsilon_2 = 10^{-6}$. In Fig. 6(a) we compare the numerical solution and exact solution, and the numerical error is plotted in Fig. 6(b). The accuracy is in the order of 10^{-2}, even we use $\Delta x = 0.05$ for this highly singular problem. The maximum error of our numerical solution is 6.61×10^{-2}.

Then, we consider a more singular case with $\varepsilon = 10^{-4}$ of this example. We apply the NGPS method in Section 6.2 to integrate Eq. (89) of this example with the following parameters: $\Delta x = 1/80$ (i.e. $n = 80$), $\rho = 200$, $h = 1$, and $\varepsilon_2 = 5\times10^{-3}$. After 147 iterations the steady-state solution is obtained. In Fig. 7(a) we compare the numerical solution and exact solution, and the numerical error is plotted in Fig. 7(b). The accuracy is also in the order of 10^{-2}. The maximum error of our numerical solution is 1.09×10^{-2}. In order to compare our numerical solutions with that calculated by Ilicasu and Schultz (2004),

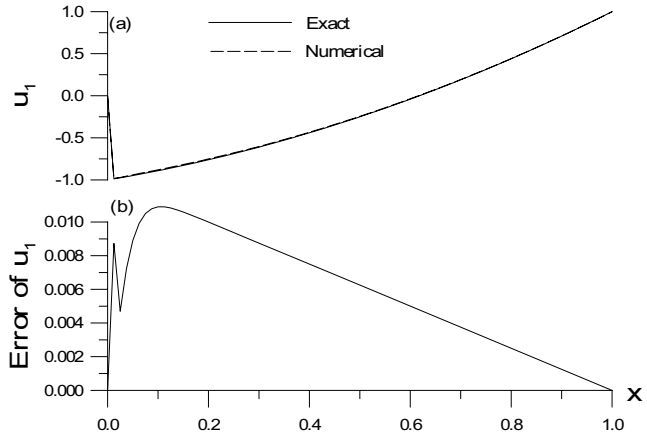

Figure 7 : For Example 2 with $\varepsilon = 0.0001$ solved by the NGPS: (a) comparing the numerical and exact solutions, and (b) the numerical error.

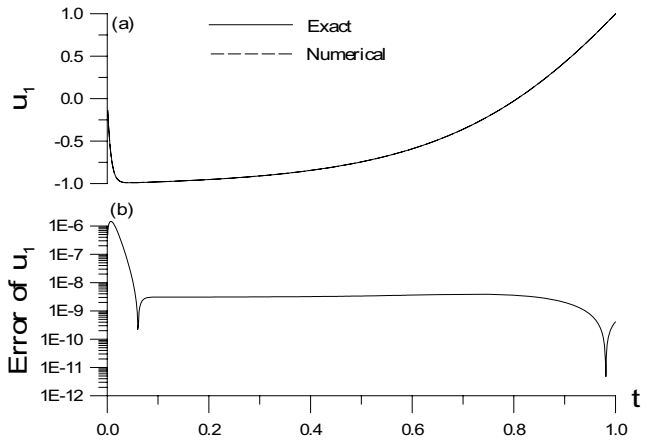

Figure 8 : For Example 2 with $\varepsilon = 0.001$ solved by the shooting method: (a) comparing the numerical and exact solutions, and (b) the numerical error.

Table 2 : For Example 2 we comparing the maximum errors for different ε and n with that of Ilicasu and Schultz (2004) denoted as IS.

ε	n	IS	NGPS
10^{-3}	20	0.82×10^{0}	6.61×10^{-2}
10^{-3}	80	0.45×10^{0}	3.42×10^{-2}
10^{-3}	200	0.14×10^{0}	9.90×10^{-3}
10^{-4}	20	0.94×10^{0}	4.87×10^{-2}
10^{-4}	80	0.92×10^{0}	1.09×10^{-2}
10^{-4}	200	0.82×10^{0}	9.14×10^{-3}

.

we also calculated the other four cases with different n, the results of which are summarized in Table 2. It can be seen that the maximum errors are reduced one or two orders by the NGPS method.

The above NGPS method is very effective even the number of grid points is small. However, the accuracy is not so good as to be compared with the shooting method.

Next we compute the case with the same stepsize $h = 10^{-3}$ for $\varepsilon = 10^{-3}$ as that used by Reddy and Chakravarthy (2004). Integrating this case by the RK4 requires smaller stepsize than that by the NGPS method. In this calculation we apply the shooting method in Section 4 and the RK4 method to the resulting $(\mathbf{y},t)$-IVP by choosing $\lambda = 2$ and $c = 500$. Through some trials we have selected $r = 0.513468817$. When compared the estimated A with the exact one $u_2(0)$ obtained from the closed-form solution in the t-domain, the error is very small with 6.96×10^{-8}. At the same time, the final value of u_1 matches very well with the exact value with an error 4.1×10^{-10}.

By using the above estimated initial condition of $u_2(0) = A$ and the given $u_1(0) = 0$, we can integrate the $(\mathbf{y},t)$-IVP by the RK4 method. In Fig. 8(a) we plot the numerical and exact solutions, which are almost coincident. Thus, we plot the numerical error in Fig. 8(b), which can be seen in the order of 10^{-6}. Obviously, our maximum error is much smaller than that calculated by Reddy and Chakravarthy (2004). When compared with the error calculated by the NGPS method as shown in Fig. 6(b) which being accurate in the first-order, the shooting method can achieve a more accurate result in the second-order. Due to the singularity, the integration by RK4 does not preserve the fourth-order accuracy with 10^{-12} and with a maximum error 1.473×10^{-6}. After the transition layer the accuracy returns to the order of 10^{-9}.

7.3 Example 3

We calculate the third example given by

$$\varepsilon u_1'' + u_1' - u_1 = 0, \tag{97}$$

$$u_1(0) = 1, \;\; u_1(1) = 1. \tag{98}$$

This example has been calculated by Reddy and Chakravarthy (2004) and Ilicasu and Schultz (2004) with

different methods.

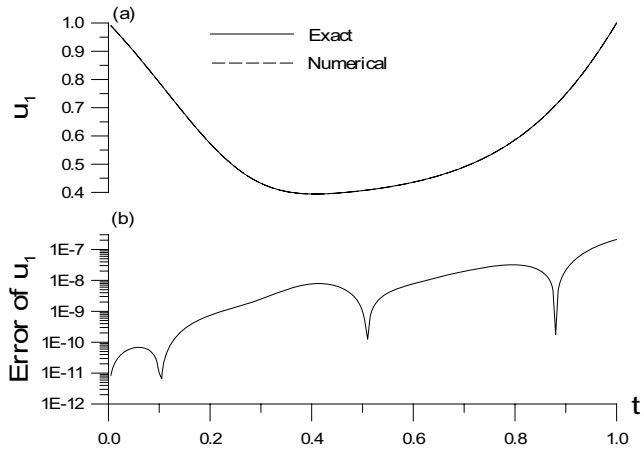

Figure 9 : For Example 3 with $\varepsilon = 0.01$ solved by the shooting method: (a) comparing the numerical and exact solutions, and (b) the numerical error.

In order to compare our numerical results with that of the above cited papers, we fix $\varepsilon = 0.01$. The translation constant $c = 5$ is also fixed.

We apply the shooting method in Section 4 and the RK4 method to the resulting $(\mathbf{y},t)$-IVP. Through some trials we have picked up the parameter r to be $r = 0.285266522$. When compared the estimated $A = -1.8770432336$ with the exact one $u_2(0) = -1.8770432329$ obtained from the closed-form solution:

$$u_1(x) = \frac{1}{e^{m_2} - e^{m_1}}[(e^{m_2} - 1)e^{m_1 x} + (1 - e^{m_1})e^{m_2 x}], \quad (99)$$

where

$$m_1 = \frac{-1 + \sqrt{1 + 4\varepsilon}}{2\varepsilon}, \ \ m_2 = \frac{-1 - \sqrt{1 + 4\varepsilon}}{2\varepsilon}, \quad (100)$$

in the t-domain, the error is very small with 7×10^{-10}. At the same time, the final value of u_1 matches very well with the exact value with an error 2.095×10^{-7}.

By using the above estimated initial condition of $u_2(0) = A$ and the given $u_1(0) = 1$, we can integrate the $(\mathbf{y},t)$-IVP by the RK4 method with a stepsize $h = 0.005$, which is the same as that used by Varner and Choudhury (1998). In Fig. 9(a) we plot the numerical and exact solutions, which are almost coincident. Thus, we plot the numerical errors in Fig. 9(b), which can be seen in the order of 10^{-7}. Obviously, our maximum error is much smaller than that calculated by Varner and Choudhury (1998), and that by Reddy and Chakravarthy (2004), of which a smaller stepsize $h = 0.001$ was used.

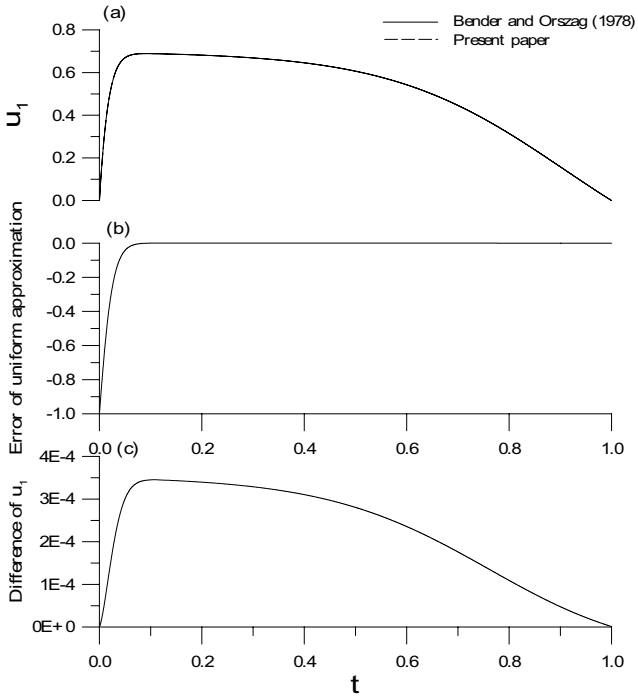

Figure 10 : For Example 4 with $\varepsilon = 0.001$ solved by the shooting method: (a) comparing the numerical solution with the uniform approximation, (b) plotting the error of uniform approximation, and (c) the difference of solutions.

7.4 Example 4

In order to further demonstrate the usefulness of the present method, let us calculate the following example of nonlinear singular perturbation problem from Bender and Orszag (1978):

$$\varepsilon u_1'' + 2u_1' + e^{u_1} = 0, \quad (101)$$

$$u_1(0) = 0, \ \ u_1(1) = 0. \quad (102)$$

This example has been also calculated by Reddy and Chakravarthy (2004).

For the comparison purpose we write the uniform approximation provided by Bender and Orszag (1978) as

$$u_1(x) = \ln \frac{2}{1+x} - e^{-2x/\varepsilon} \ln 2. \quad (103)$$

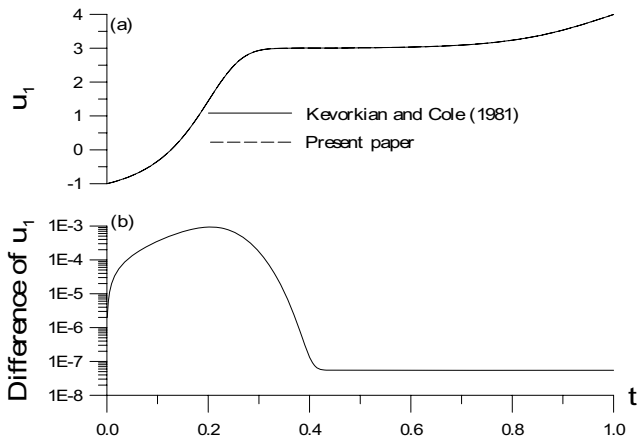

Figure 11 : For Example 5 with $\varepsilon = 0.001$ solved by the shooting method: (a) comparing the numerical solution with the uniform approximation, and (b) the difference of solutions.

When the singular parameter is taken to be $\varepsilon = 0.001$, we apply the shooting method in Section 4 and the RK4 method to the resulting $(\mathbf{y},t)$-IVP under $\lambda = 3$ and $c = -2$. Through some trials we have picked up $r = 0.6013428$. By using a stepsize $h = 0.0001$ the numerical result and the solution in Eq. (103) are compared in Fig. 10(a). We insert Eq. (103) into Eq. (101) to obtain

$$\varepsilon u_1'' + 2u_1' + e^{u_1} = \frac{\varepsilon}{(1+x)^2} + \frac{2^{[1-e^{-2x/\varepsilon}]} - 2}{1+x}. \tag{104}$$

The error to satisfy Eq. (101) is plotted in Fig. 10(b) in the t-domain. In addition that very near the left-hand boundary with $x \le 0.00326814$, the error is very small in the order of 10^{-4}. The difference between our numerical result with the solution in Eq. (103) is also plotted in Fig. 10(c), of which the absolute difference is smaller than 3.45×10^{-4}. This example shows that the new method is also applicable to the nonlinear problem.

7.5 Example 5

Finally, we consider the following example of nonlinear singular perturbation problem from Kevorkian and Cole (1981):

$$\varepsilon u_1'' + u_1 u_1' - u_1 = 0, \tag{105}$$

$$u_1(0) = -1, \;\; u_1(1) = 3.9995. \tag{106}$$

For comparison purpose we write the uniform approximation provided by Kevorkian and Cole (1981) as

$$u_1(x) = x + c_1 \tanh[c_1(x/\varepsilon + c_2)/2], \tag{107}$$

where $c_1 = 2.9995$ and $c_2 = 1/c_1 \ln[(c_1-1)/(c_1+1)]$.

When the singular parameter is taken to be $\varepsilon = 0.001$, we apply the shooting method to the resulting $(\mathbf{y},t)$-IVP under $\lambda = 5$ and $c = 5$. Through some trials we used $r = 0.10880495$. The numerical result matches very well the boundary condition $u_1(1) = 3.9995$ with a very small error with 5.48×10^{-8}. By using a stepsize $h = 0.0001$ the numerical result and the solution in Eq. (107) are compared in Fig. 11(a). The absolute difference between our numerical result with the solution in Eq. (107) is also plotted in Fig. 11(b), of which the difference of our solution with the solution in Eq. (107) is smaller than 10^{-3}. This example has been also calculated by Reddy and Chakravarthy (2004) under the same $\varepsilon = 0.001$ as shown in Table 5 therein. Near the boundary layer the solution obtained by Reddy and Chakravarthy (2004) deviates from the uniformly valid approximation (107) to a great extent with the difference 0.493912

For this problem, Wang (2004) has obtained a different solution by a series method:

$$u_1(x) = x + 2.9995 + \frac{L(s)}{Q(s)}, \tag{108}$$

where $s = x/\varepsilon$ is a strained coordinate, and

$$\begin{aligned} L(s) = {} & -3.9995 + (1.99975 + c_3)s - 0.39995(1+2c_3)s^2 \\ & + [0.0333292(1+2c_3) - 0.25c_3 + 0.1c_3(1+2c_3) \\ & + 0.166667(c_3 - c_3^2)]s^3, \end{aligned} \tag{109}$$

$$\begin{aligned} Q(s) = {} & 1 - 0.5s + 0.1(1+2c_3)s^2 \\ & - 0.0083333(1+2c_3)s^3, \end{aligned} \tag{110}$$

where $c_3 = -1.999791999$.

When the singular parameter is taken to be very small with $\varepsilon = 10^{-6}$, we apply the shooting method to the resulting $(\mathbf{y},t)$-IVP under $\lambda = 6$ and $c = 10$. Through some trials we used $r = 0.61685$. By using a stepsize $h = 10^{-6}$ the numerical result and the solutions in Eqs. (107) and (108) are compared in Fig. 12(a). The result obtained by Wang (2004) as shown by the dashed-dotted line deviates much from our solution and the solution of Kevorkian

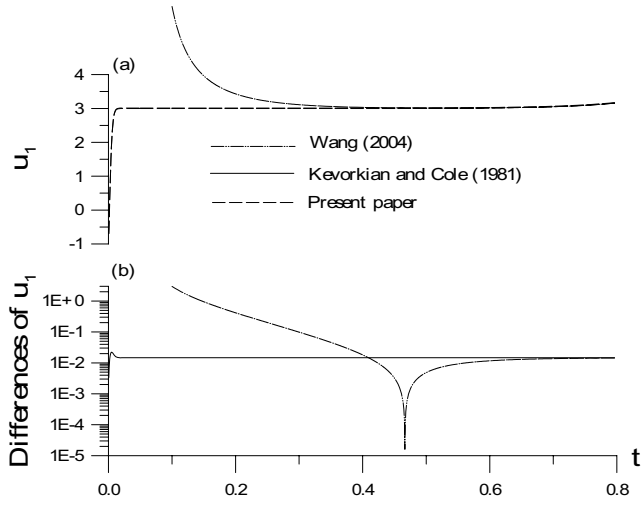

Figure 12 : For Example 5 with $\varepsilon = 0.000001$ solved by the shooting method: (a) comparing the numerical solution with the uniform approximations, and (b) the differences of solutions.

and Cole (1981) when $t < 0.4$, i.e., $x < 1.4798 \times 10^{-3}$. It indicates that the solution of Wang (2004) cannot match the boundary layer solution.

The difference between our numerical result with the solution in Eq. (107) is plotted in Fig. 12(b), of which the difference is smaller than 2×10^{-2}. The difference between our numerical result with the solution in Eq. (108) is also plotted in Fig. 12(b) with the dashed-dotted line, of which it can be seen that the error of the solution of Wang (2004) increases very fast when near the boundary layer. Obviously, the solution of Wang (2004) needs more higher-order terms in the expansions of Eqs. (108)-(110) to match the boundary layer behavior.

This example shows again that the new method is also applicable to the nonlinear singular perturbation problem with high singularity.

8 Conclusions

For its very nature of singularity, in the open literature there is no or rare report that one can directly use the shooting method as a technique to solve the SPBVP. In order to reduce the singularity this paper has employed a coordinate transformation from the x-domain problem to the t-domain problem. The relation between singularity and stiffness is then demonstrated, of which the coordinate transformation parameter λ plays a key role to balance these two tendencies. For a stabilization of the newly developed method we also introduced the new systems by a translation of the dependent variable. Therefore, this paper has identified four systems, namely, the $(\mathbf{u},x)$-BVP, the $(\mathbf{u},t)$-IVP, the $(\mathbf{y},x)$-BVP or IVP, and the $(\mathbf{y},t)$-IVP.

In order to estimate the missing initial condition for the singularly perturbed boundary value problems expressed as the $(\mathbf{y},t)$-IVPs, we have employed the Lie group method to derive algebraic equations. Therefore, we can determine r very quickly only through a few trials. Five numerical examples, three linear and two nonlinear, were calculated by the new method. Compared with other numerical methods, the new approach displays its high efficiency and high accuracy. The numerical results have the second-order accuracy even for the highly singular cases.

This paper also developed a finite difference method together with the nonstandard group preserving scheme to calculate the SPBVPs. This method is suitable for the calculation of SPBVPs without needing for many grid points; however, its accuracy is of the first-order.

Although the Lie-group shooting method can estimate the missing initial condition very accurately, and in principle, the RK4 has the fourth-order accuracy, the accuracy of numerical solutions integrated by RK4 is reduced since the resultant $(\mathbf{y},t)$-IVPs exhibit certain stiffness. To remedy this defect, we may consider the implicit-form RK4 stiff integrator in a forthcoming study. In view of the results in [Liu (2006b)], the present approach may be improved such that the iterative solution of the missing initial condition can be avoided.

Here, we only considered the boundary layer located at the left-hand side. In the future it is deserved to extend the new method to more complex singularly perturbed problems, of which there may appear two-layer, interior layer or spike layer as that for the Carrier-Pearson problem (Carrier and Pearson, 1991).

Acknowledgement: The author would like to acknowledge the research sponsor by the National Science Council of Taiwan under the grant NSC 95-2221-E-019-002.

9 References

Ascher, U. M.; Mattheij, R. M. M.; Russell, R. D. (1995): Numerical Solution of Boundary Value Problems for Ordinary Differential Equations. SIAM, Philadelphia.

Bender, C. M.; Orszag, S. A. (1978): Advanced Mathematical Methods for Scientists and Engineers. McGraw-Hill, New York.

Carrier, G.; Pearson, C. (1991): Ordinary Differential Equations. SIAM, Philadelphia.

De Jager, E. M.; Jiang, F. R. (1996): The Theory of Singular Perturbation. Noth-Holland, Amsterdam.

Gasparo, M. G.; Macconi, M (1989): New initial-value method for singularly perturbed boundary value problems. *J. Optim. Theory Appl.*, vol. 63, pp. 213-224.

Gasparo, M. G.; Macconi, M. (1990): Initial-value methods for second-order singularly perturbed boundary value problems. *J. Optim. Theory Appl.*, vol. 66, pp. 197-210.

Ilicasu, F. O.; Schultz, D. H. (2004): High-order finite-difference techniques for linear singular perturbation boundary value problems. *Int. J. Comput. Math. Appl.*, vol. 47, pp. 391-417.

Kadalbajoo, M. K.; Patidar, K. C. (2002): A survey of numerical techniques for solving singularly perturbed ordinary differential equations. *Appl. Math. Comp.*, vol. 130, pp. 457-510.

Kadalbajoo, M. K.; Reddy, Y. N. (1986): Initial-value technique for a class of nonlinear singular perturbation problems. *J. Optim. Theory Appl.*, vol. 53, pp. 395-406.

Keller, H. B. (1992): Numerical Methods for Two-point Boundary Value Problems. Dover, New York.

Kevorkian, J.; Cole, J. D. (1981): Perturbation Methods in Applied Mathematics. Springer-Verlag, New York.

Kevorkian, J.; Cole, J. D. (1996): Multiple Scale and Singular Perturbation Methods. Springer-Verlag, New York.

Kubicek, M.; Hlavacek, V. (1983): Numerical Solution of Nonlinear Boundary Value Problems with Applications. Prentice-Hall, New York.

Li, Z.; Wang, W. (2005): Mechanization for solving SPP by reducing order method. *Appl. Math. Comput.*, vol. 169, pp. 1028-1037.

Liu, C.-S. (2001): Cone of non-linear dynamical system and group preserving schemes. *Int. J. Non-Linear Mech.*, vol. 36, pp. 1047-1068.

Liu, C.-S. (2005): Nonstandard group-preserving schemes for very stiff ordinary differential equations. *CMES: Computer Modeling in Engineering & Sciences*, vol. 9, pp. 255-272.

Liu, C.-S. (2006a): Preserving constraints of differential equations by numerical methods based on integrating factors. *CMES: Computer Modeling in Engineering & Sciences*, vol. 12, pp. 83-108.

Liu, C.-S. (2006b): The Lie-group shooting method for nonlinear two-point boundary value problems exhibiting multiple solutions. *CMES: Computer Modeling in Engineering & Sciences*, vol. 13, pp. 149-163.

Liu, C.-S. (2006c): One-step GPS for the estimation of temperature-dependent thermal conductivity. *Int. J. Heat Mass Transf.*, vol. 49, pp. 3084-3093.

Liu, C.-S. (2006d): An efficient simultaneous estimation of temperature-dependent thermophysical properties. *CMES: Computer Modeling in Engineering & Sciences*, vol. 14, pp. 77-90.

Liu, C.-S. (2006e): An efficient backward group preserving scheme for the backward in time Burgers equation. *CMES: Computer Modeling in Engineering & Sciences*, vol. 12, pp. 55-65.

Liu, C.-S. (2006f): A group preserving scheme for Burgers equation with very large Reynolds number. *CMES: Computer Modeling in Engineering & Sciences*, vol. 12, pp. 197-211.

Liu, C.-S.; Chang, C.-W.; Chang, J.-R. (2006): Past cone dynamics and backward group preserving schemes for backward heat conduction problems. *CMES: Computer Modeling in Engineering & Sciences*, vol. 12, pp. 67-81.

Natesan, S.; Ramanujam, M. (1998): Initial-value technique for singularly-perturbed turning-point problems exhibiting twin boundary layers. *J. Optim. Theory Appl.*, vol. 99, pp. 37-52.

Nayfeh, A. H. (1981): Introduction to Perturbation Techniques. Wiley, New York.

O'Malley, R. E. (1991): Singular Perturbation Methods for Ordinary Differential Equations. Spring-Verlag, New York.

Reddy, Y. N.; Chakravarthy, P. P. (2004): An initial-value approach for solving singularly perturbed two-

point boundary value problems. *Appl. Math. Comput.*, vol. 155, pp. 95-110.

Roberts, S. M. (1982): A boundary-value technique for singular perturbation problems. *J. Math. Anal. Appl.*, vol. 87, pp. 489-503.

Roos, H. G.; Stynes, M.; Tobiska, L. (1996): Numerical Methods for Singularly Perturbed Differential Equations. Spring-Verlag, Berlin.

Shampine, L. F.; Gear, C. W. (1979): A user's view of solving stiff ordinary differential equations. *SIAM Rev.*, vol. 21, pp. 1-17.

Varner, T. N.; Choudhury, S. R. (1998): Non-standard difference schemes for singular perturbation problems revisited. *Appl. Math. Comput.*, vol. 92, pp. 101-123.

Wang, L. (2004): A novel method for a class of nonlinear singular perturbation problems. *Appl. Math. Comput.*, vol. 156, pp. 847-856.